RESEARCH ARTICLE | DECEMBER 10 2018

Numerical pricing of options under the exponential Ornstein–Uhlenbeck stochastic volatility model based on a DG technique FREE

J. Hozman ✉; T. Tichý

AIP Conf. Proc. 2048, 030012 (2018)
https://doi.org/10.1063/1.5082070

Numerical Pricing of Options under the Exponential Ornstein–Uhlenbeck Stochastic Volatility Model based on a DG Technique

J. Hozman[1,a)] and T. Tichý[2,b)]

[1]*Faculty of Science, Humanities and Education, Technical University of Liberec, 461 17 Liberec, Czech Republic*
[2]*Faculty of Economics, VŠB – Technical University of Ostrava, 701 21 Ostrava, Czech Republic*

[a)]Corresponding author: jiri.hozman@tul.cz
[b)]tomas.tichy@vsb.cz

Abstract. Stochastic volatility models are a variance extension of the classical Black-Scholes model dynamics by introducing another auxiliary processes to model the volatility of the underlying asset returns. Here we study the pricing problem for European-style options under a one-factor stochastic volatility model when the volatility of the underlying price is governed by the exponential Ornstein–Uhlenbeck process. The problem can be formulated as a non-stationary second-order degenerate partial differential equation accompanied by initial and boundary conditions, whose analytical solutions are not available in general. Therefore, the approximate option value is obtained by a numerical procedure based on a discontinuous Galerkin technique that provides promising results. Finally, reference numerical experiments are provided with the emphasis on the behaviour of the option values with respect to the discretization parameters.

INTRODUCTION

As the general foundations of modern theory of option pricing we generally accept the ideas published by Black and Scholes [1] and Merton [2], i.e., construction of a riskless portfolio consisting of a given option and its underlying asset (or, potentially, further risk sources). The aforementioned authors found out that the solution of the problem was closely related to the solution of the heat equation well known in physics, i.e., partial differential equation (PDE) with proper boundary and terminal (initial) conditions. This finding provides valuable evidence of applicability of a particular method within various fields of science.

However, since the system can lead to analytical option pricing formula only under some simplifying assumptions, it is often inevitable to adopt some of the numerical approximation techniques. Among the assumptions that are not fulfilled by empirical observations of option underlying asset returns, we can name especially the Gaussianity of log-returns and their constant volatility. It therefore follows that the market participants need sufficient knowledge of advanced mathematical methods so that a fair price, i.e., a no-arbitrage price, of a given option can be discovered.

In the late 1980s many empirical studies led us to relax the idealized assumption of a constant volatility of the underlying asset returns as postulated by Black and Scholes in their seminal work [1]. This generalization of Black–Scholes (BS) framework resulted in advanced option pricing models that show much better performance and are valid for realistic parameters reflected by the empirical observations.

In this contribution we focus on a numerical solution of the option pricing problem using the discontinuous Galerkin (DG) technique as an alternative to the common approaches based on finite differences [3] and elements [4]. Although the DG method was developed in the early 1970s and it was successfully profiled in the field of computational fluid dynamics, see [5, 6], its potency in option pricing problems has not yet been fully exploited. While finite difference or element methods are frequently discussed in the literature, relatively little can be found for the modern pricing techniques. Apart from the DG method cite at least the recent wavelet approach [7] following paper [8] and also mention work [9], which uses a wavelet basis [10] in the Galerkin method for solving the second-order PDEs with an appropriate post-processing. In particular, our aim is addressed to extend the concept of the DG technique

Proceedings of the 44th International Conference on Applications of Mathematics in Engineering and Economics
AIP Conf. Proc. 2048, 030012-1–030012-8; https://doi.org/10.1063/1.5082070
Published by AIP Publishing. 978-0-7354-1774-8/$30.00

for a wide range of one-factor stochastic volatility models for pricing of European-style options, from the Heston model [11], over the Stein–Stein model [12] to the Scott model [13].

We proceed as follows. First, we recall the exponential Ornstein–Uhlenbeck stochastic volatility model as a modification of the Scott model, which relaxes the assumption of a constant volatility. This model considered is represented as a pricing equation defined in the bounded space-time domain. Subsequently, we recall a numerical algorithm based on spatial and temporal discretizations from [14] and show numerical results capturing the behaviour of the option values with respect to the discretization parameters.

EXPONENTIAL ORNSTEIN–UHLENBECK STOCHASTIC VOLATILITY MODEL

The non-deterministic behaviour of the volatility parameter is usually ensured by introducing another auxiliary process to the model. In the model presented the volatility is driven by an exponential Ornstein–Uhlenbeck (expOU) process, in particular for its ability to capture a volatility clustering, a leverage effect and a volatility autocorrelation standardly observed in real market data. The expOU model is a slight modification of the stochastic volatility model firstly introduced by L.O. Scot in [13]. The model dynamics is governed by a pair of Itô stochastic differential equations

$$dS_{\tilde{t}} = \mu S_{\tilde{t}} d\tilde{t} + \sqrt{k_S \exp(Y_{\tilde{t}})}\, S_{\tilde{t}} dW_{\tilde{t}}, \quad S_0 \geq 0, \tag{1}$$

$$dY_{\tilde{t}} = \alpha(m - Y_{\tilde{t}})d\tilde{t} + \beta\, dZ_{\tilde{t}}, \quad Y_0 \geq 0, \tag{2}$$

where $S_{\hat{t}}$ and $Y_{\hat{t}}$ are the price of the underlying asset and the value of the auxiliary quantity related to a volatility at actual time $\hat{t}$. The symbols $W_{\tilde{t}}$ and $Z_{\tilde{t}}$ denote two correlated Wiener processes with factor ρ that takes values in $[-1, 1]$. The system (1)–(2) is calibrated with several fixed constants, namely: $\mu \in \boldsymbol{R}$, an expected growth rate of the asset price; $\alpha > 0$, a rate of mean reversion; $m \geq 0$, a long term mean of the volatility process; $\beta > 0$ a volatility of volatility parameter (vol-of-vol). For a detailed explanation of these market parameters the reader is referred to the book [15]. It is important to mention that volatility is determined by a square root of $k_S \exp(Y)$, where the parameter k_S plays a role as a scaling factor to be able to cover different volatility scales, see (1). Finally, we remark that supposing an uncorrelated case ($\rho = 0$) and swapping k_S^2 and $2Y$ for k_S and Y in (1), then one receives the original Scott model from [13].

Next, we consider a European-style option on the financial asset S with the stochastic volatility related to the driving process Y, whose dynamics are given by (1) and (2), respectively. Such an option is possible to exercise only at maturity time T and it exists either as a put that gives the holder the right to sell an underlying asset for an agreed strike price $\mathcal{K}$, or as a call that allows him or her to buy it for this strike. Therefore, the option values can be represented as a function $V = V(S, Y, t)$ of the underlying asset price S, the volatility process Y and the time to maturity $t = T - \hat{t}$.

Similarly to the BS framework, the option V is priced using an approach based on no arbitrage principle, Itô stochastic calculus and a construction of a riskless portfolio (with a constant risk-free interest rate $r \geq 0$), see the procedure in a more detail in [14]. Then, we obtain a generalized Black–Scholes type PDE model for pricing European-style options under a single factor stochastic volatility governed by the exponential Ornstein–Uhlenbeck process, i.e., the pricing PDE is as follows

$$\frac{\partial V}{\partial t} - \frac{1}{2} k_S \exp(Y) S^2 \frac{\partial^2 V}{\partial S^2} - rS\frac{\partial V}{\partial S} + rV - \rho\beta\sqrt{k_S}\exp(Y/2) S \frac{\partial^2 V}{\partial S\, \partial Y} - \frac{1}{2}\beta^2 \frac{\partial^2 V}{\partial Y^2} - \Big(\alpha(m - Y) - \beta\Lambda(S, Y, t)\Big)\frac{\partial V}{\partial Y} = 0 \tag{3}$$

for $S > 0$, $Y \in \boldsymbol{R}$ and $0 < t \leq T$.

The function $\Lambda(S, Y, t)$ in (3) defines the so-called market price of the volatility risk and it has a specific form for the particular stochastic volatility models, cf. [11] and [12]. We remark that we consider $\Lambda(S, Y, t) = 0$ in the rest of the paper to simplify the problem analysis. Although here it may seem that this setting is not quite realistic from a financial point of view; for the comparison with the reference stochastic models [13] and [16], zero market price of the volatility risk is reasonable in case that we can assume that the volatility risk is hedgeable.

Since the pricing equation (3) is of the first order in time, it is necessary to prescribe the initial condition given by the payoff function of the corresponding European vanilla option at maturity date T, i.e.,

$$V(S(0), Y(0), 0) = \begin{cases} \max(S - \mathcal{K}, 0), & \text{if } V \text{ is a call option,} \\ \max(\mathcal{K} - S, 0), & \text{if } V \text{ is a put option.} \end{cases} \tag{4}$$

Pricing Equation on the Bounded Domain

Although, the option pricing problem (3) with initial state (4) is defined on the unbounded spatial domain, the numerical treatment has to be performed on the bounded space-time domain.

At first, we introduce the change of variables and the unknown. From the financial point of view the relation $S \gg Y$ is very common, thus it is convenient in what follows to use the scaled asset prices and options values, i.e.,

$$x = [x_1, x_2] = [S/\mathcal{K}, Y], \quad u(x,t) = V(S,Y,t)/\mathcal{K}, \quad u(x,0) = \begin{cases} \max(x_1 - 1, 0), & \text{for a call option,} \\ \max(1 - x_1, 0), & \text{for a put option,} \end{cases} \tag{5}$$

Secondly, we restrict the option pricing problem to a bounded rectangular domain $\Omega = (0, S_{max}/\mathcal{K}) \times (-Y_{max}, Y_{max})$, where S_{max} stands for the maximal price of the underlying asset and $Y_{max} > 0$ related to the volatility of asset returns is large enough (see boundary conditions).

Further, using the chain rule in (3), we obtain a new pricing equation for the function $u(x,t) : \Omega \times (0,T) \to [0, +\infty)$, namely

$$\frac{\partial u}{\partial t} - \nabla \cdot (\boldsymbol{D}(x) \cdot \nabla u) + \nabla \cdot \left(\vec{b}(x)\, u\right) + c(x)\, u = 0 \quad \text{in } \Omega \times (0,T) \tag{6}$$

with the symmetric positive semi-definite matrix

$$\boldsymbol{D}(x) = \frac{1}{2} \begin{pmatrix} k_S\, x_1^2 \exp(x_2) & \rho\beta \sqrt{k_S}\, x_1 \exp(x_2/2) \\ \rho\beta \sqrt{k_S}\, x_1 \exp(x_2/2) & \beta^2 \end{pmatrix}, \tag{7}$$

the vector field

$$\vec{b}(x) = (b_1(x), b_2(x))^T = \left(\left(k_S \exp(x_2) + \rho\beta \sqrt{k_S} \exp(x_2/2)/4 - r\right) x_1,\ \rho\beta \sqrt{k_S} \exp(x_2/2)/2 - \alpha(m - x_2) \right)^T \tag{8}$$

and the scalar function

$$c(x) = 2r - \alpha - k_S \exp(x_2) - \rho\beta \sqrt{k_S} \exp(x_2/2)/2. \tag{9}$$

The governing equation (6) restricted to the space-time domain $\Omega \times (0,T)$ is equipped with the initial condition (5) and it has to be additionally supplemented by the suitable boundary conditions on appropriate parts of the boundary $\partial\Omega$ to preserve the well-posed problem formulation. In order to ensure the theoretical accuracy of the numerical approximations, the setting of boundary conditions plays a crucial role and has to be done in a more rigorous way to be in the accordance with the degeneracy of (6) and with the flow determined by the vector field (8), for a detailed explanation see [17].

In what follows, we split the boundary $\partial\Omega$ on four disjoint parts

$$\Gamma_1 = (0, S_{max}/\mathcal{K}) \times \{-Y_{max}\},\ \Gamma_2 = \{S_{max}/\mathcal{K}\} \times (-Y_{max}, Y_{max}),\ \Gamma_3 = (0, S_{max}/\mathcal{K}) \times \{Y_{max}\},\ \Gamma_4 = \{0\} \times (-Y_{max}, Y_{max}) \tag{10}$$

and prescribe the mixed boundary conditions in the following form

- on $\Gamma_1 \cup \Gamma_3$: By choosing Y_{max} sufficiently large the far-field boundaries with respect to Y variable lie outside the zone of the practical interest, in which option values are desirable to know. More precisely, if $b_2(x) < 0$ on $Y = -Y_{max}$ and $b_2(x) > 0$ on $Y = Y_{max}$, then the setting of artificial boundary conditions does not affect the solution in the zone of the financial interest. Therefore, we prescribe here the Dirichlet boundary condition that involves an extrapolation u_{ext} of the option value from the interior of Ω onto the corresponding parts of the boundary, i.e.,
$$u(x,t) = u_{ext}(x,t) \quad \text{on } \Gamma_1 \cup \Gamma_3,\ t > 0. \tag{11}$$
- on Γ_2: According to [14] we prescribe the Neumann boundary condition corresponding to asymptotic slopes of plain vanilla options as $S \to +\infty$, i.e.,
$$\frac{\partial u}{\partial x_1}(x,t) = \begin{cases} 1, & \text{for a call option,} \\ 0, & \text{for a put option,} \end{cases} \quad \text{on } \Gamma_2,\ t > 0. \tag{12}$$
- on Γ_4: On line $S = 0$, the spatial derivative terms with respect to S variable vanish in (3) and the pricing equation degenerates. Therefore, no boundary condition has to be imposed on the boundary Γ_4, see also $b_1(x) = 0$ in [17].

The resulting pricing equation (6) is closely related to the convection–diffusion equation, which exhibits a parabolic and hyperbolic behaviour in dependency on a proportion of the terms (7) and (8). Therefore, to solve this problem the DG technique is employed, which is widely and successfully used in the field of the convection–diffusion problems.

NUMERICAL ALGORITHM

We employ a numerical algorithm to the pricing equation (6) equipped with the initial and boundary conditions. This algorithm consists of two consecutive phases — DG space semi-discretization and Crank–Nicolson time discretization.

Within the first phase, we construct the semi-discrete solution $u_h = u_h(t)$, $t \in [0, T]$, from the finite dimensional space S_h^p of discontinuous piecewise polynomial functions of the p-th order defined on the triangulation $\mathcal{T}_h$ of domain Ω with a mesh parameter h, see the DG framework in [6]. Based on similar techniques, cf. [18], this semi-discrete solution is defined using a method of lines leading to the system of the ordinary differential equations as follows

$$\frac{d}{dt}\,(u_h, v_h) + \mathcal{A}_h(u_h, v_h) = l_h(v_h)(t) \quad \forall\, v_h \in S_h^p,\ \forall\, t \in (0, T), \tag{13}$$

where the initial condition $u_h(0)$ is given by (5), $(\cdot, \cdot)$ denotes the inner product in $L^2(\Omega)$, the bilinear form $\mathcal{A}_h(\cdot, \cdot)$ stands for the DG semi-discrete variant of the degenerate parabolic partial differential operator from (6), accompanied with penalties and stabilizations, and the form $l_h(\cdot)(t)$ balances boundary conditions, for more details see [14].

The second phase aims to discretize the problem (13) on the time interval with a time step τ by the Crank–Nicolson method to obtain the numerical algorithm of a high accuracy with respect to both discretization parameters. Setting $\{\varphi_i\}_{i=1}^{DOF}$ as a basis of space S_h^p, then one can easily identify the approximate solution u_h at each time level $t_m \in [0, T]$ with the vector of real coefficients $U_m \in \boldsymbol{R}^{DOF}$ appearing in the linear combination of basis functions. This unknown vector U_m is sought as a solution of the following sparse linear algebraic problems

$$\left(\mathbf{M} + \frac{\tau}{2}\,\mathbf{A}\right) U_{m+1} = \left(\mathbf{M} - \frac{\tau}{2}\,\mathbf{A}\right) U_m + \frac{\tau}{2}\,(F_{m+1} + F_m), \quad m = 0, 1, \ldots \tag{14}$$

with starting data U_0 related to the payoff function (5), see, e.g., [19]. The mass matrix $\mathbf{M}$ and the matrix $\mathbf{A}$ arising from the bilinear form $\mathcal{A}_h$ are defined as follows

$$\mathbf{M} = \Big\{(\varphi_j, \varphi_i)\Big\}_{i,j=1}^{DOF}, \qquad \mathbf{A} = \Big\{\mathcal{A}_h(\varphi_j, \varphi_i)\Big\}_{i,j=1}^{DOF}. \tag{15}$$

and the right-hand side of (14) contains an average of two vectors

$$F_m = \{l_h(\varphi_i)(t_m)\}_{i=1}^{DOF}, \qquad F_{m+1} = \{l_h(\varphi_i)(t_{m+1})\}_{i=1}^{DOF}, \tag{16}$$

enforcing the fulfillment of boundary conditions at the corresponding time levels. The solvability of the sparse linear algebraic system (14) is proven in [14].

NUMERICAL RESULTS

In the forthcoming paragraphs, we want to illustrate the potency of the DG technique to pricing of European-style options under the exponential Ornstein–Uhlenbeck stochastic volatility model. The presented numerical algorithm is implemented in solver Freefem++ [20] and computations are preformed with piecewise linear ($p = 1$), quadratic ($p = 2$) and cubic ($p = 3$) approximations on uniformly structured and adaptively refined triangular meshes to resolve well the obtained numerical solution in the whole computational domain. Regarding to the temporal discretization, we assume that there are 360 days in a year, thus the time step is set proportional to one calendar day, i.e., $\tau = 1/360$. This length of the time step is sufficient and taking another smaller values does not improve the results significantly. Finally note that the sequence of sparse linear algebraic problems (14) is solved by GMRES solver for all simulations.

As a model benchmark we price a European put on a stock assuming stochastic volatility of stock price returns. To be consistent with the reference data [16], we consider several strikes $\mathcal{K} \in \{80, 90, 100, 110, 120, 130\}$ with short ($T = 2/12$) and middle ($T = 12/12$) maturities. The remaining model parameters are as follows

$$r = 0.0, \qquad \alpha = 3.0, \qquad m = 0.0, \qquad \beta = 1.0, \qquad k_S = 0.1\,\exp(-T/2), \qquad \rho = -0.6. \tag{17}$$

We remark that the relation $\alpha > \beta^2$ of parameters mentioned above implies that the leverage effect is slower than the volatility autocorrelation decay with a characteristic time, cf. [16]. Although, this situation is not often empirically observed in real markets, it could be still reasonable. Finally, note that ρ has to be negative just because of the leverage effect.

Next, the computational domain data S_{max} and Y_{max} are chosen sufficiently large, e.g., $S_{max} = 400$ and $Y_{max} = 1.0$, in order to the far-field boundaries lie far enough from the zone of the practical interest determined by the reference node with coordinates $S_{ref} = 100$ and $Y_{ref} = 0$.

First of all, we want to graphically capture how numerical solutions develop in the whole computational domain during simulations from a payoff function in Figure 1 to the final state in Figure 2. The depicted solutions are obtained with the presented numerical algorithm using piecewise linear approximations. In the case of a one-year simulation, the mesh is refined adaptively every 60 days, from the initial grid having 800 elements to the final one with approximately the same number of elements. This mesh refinement and smoothing of the initial state are most apparent in the neigbourhood of line $S = \mathcal{K}$, where the solution changes dramatically with respect to the direction of the vector field $\vec{b}(x)$ from (8), this fact is better observable on plots with isolines of solutions. Moreover, one can also notice that while the initial state is symmetric with respect to Y variable, the subsequent development already contains asymmetry, this is due to the exponentially driven volatility.

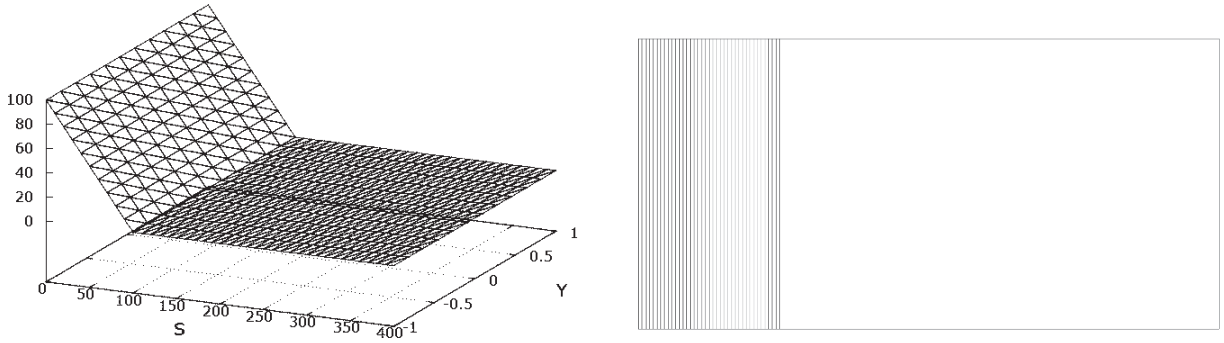

FIGURE 1. Piecewise linear approximation of the payoff function with $\mathcal{K} = 100$: 3D plot (left) and isoline plot (right).

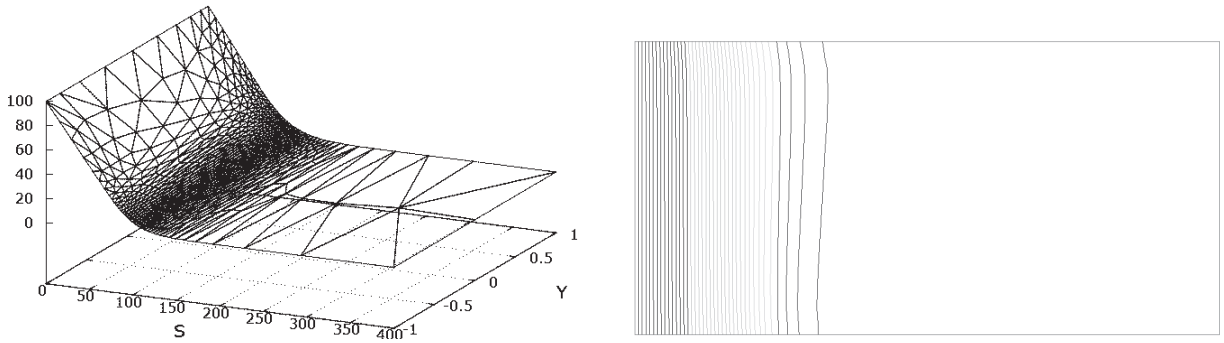

FIGURE 2. Piecewise linear approximation of one-year option prices with $\mathcal{K} = 100$: 3D plot (left) and isoline plot (right).

Secondly, our aim is to provide the deeper insight to the properties of the studied option pricing problem with respect to maturities. Therefore, we capture two scenarios with different times to maturity (two months and one year) and strike $\mathcal{K} = 100$. In Figure 3, it is apparent that approximate option prices increase as the time to maturity raises. This effect is the most evident for ATM or near ATM options and has the same character for different polynomial orders.

Further, for a complete overview, we contrast the obtained results with BS prices and evaluate the price differences between the values from the stochastic volatility model and BS framework ($\alpha = \beta = 0$) with a comparable volatility. For a particular case $\mathcal{K} = 100$ and $T = 12/12$, Figure 4 shows this relationship for fixed $Y = Y_{ref}$, where BS

prices frequently underprice and overprice the approximate option values. More precisely, in the negatively correlated case ($\rho = -0.6$), the BS prices underprice ITM puts with stochastic volatility and overprice OTM ones. Again note that the different polynomial orders do not change the conclusions above. Moreover, the behaviour observed in Figure 3 and Figure 4 is in a quite good agreement with empirical findings common for European-style options priced under the exponential Ornstein–Uhlenbeck stochastic volatility model.

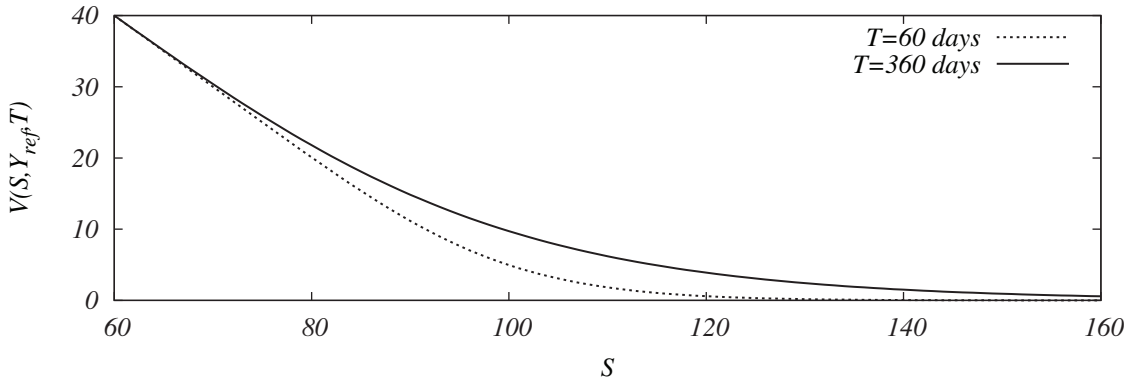

FIGURE 3. Effect of different maturities on approximate piecewise linear option prices for $Y = Y_{ref}$ and $\mathcal{K} = 100$.

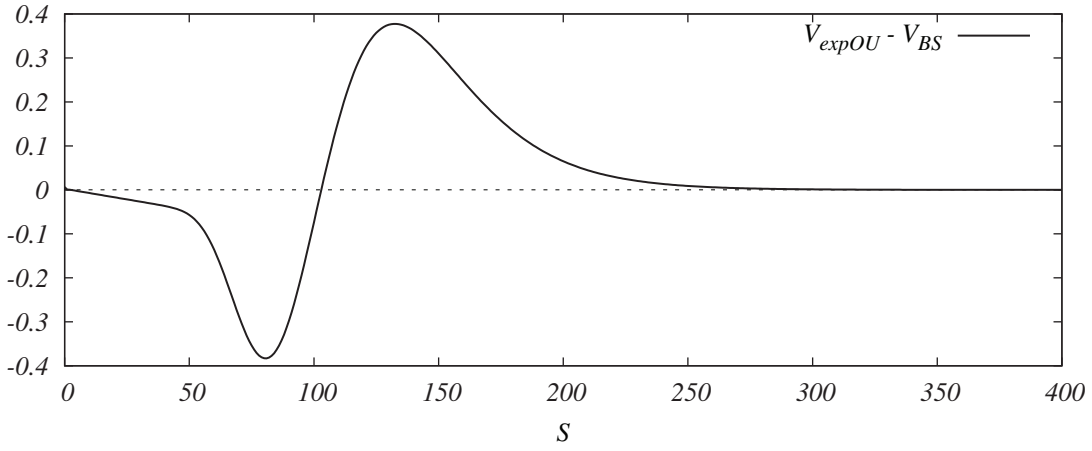

FIGURE 4. One-year option price differences between values from stochastic volatility model and BS framework with volatility of $\sqrt{k_S}$ and strike $\mathcal{K} = 100$.

The last task is to investigate the behaviour of option values with respect to the different mesh sizes h as well as polynomial orders p of approximation. We compute the piecewise linear, quadratic and cubic numerical solutions of the option pricing problem on a sequence of the consecutive refined grids. The numerical results (for each combination of h and p) are evaluated at the given reference node $[S_{ref}, Y_{ref}]$ and compared with those obtained by method from [16] using Taylor expansions. We also append the results from Monte Carlo (MC) simulation, which are considered here as reference ones.

We present several scenarios for different times to maturity and strikes. For the case of two-month maturity, the comparative results are recorded in Table 1, which is divided into three panels corresponding to the particular polynomial order. The obtained results are of a higher accuracy and usually match better the reference values as the polynomial order increases and mesh size decreases. More precisely, one can easily observe that the presented DG technique produces numerical values that are much closer to the reference prices (represented by MC values) than

results in [16]. We come to the same conclusions also for the second case with parameters describing the option with one-year maturity, see Table 2.

TABLE 1. Comparison of approximate two-month option values at reference node $[S_{ref}, Y_{ref}]$ for different scenarios, mesh sizes and polynomial orders with the reference results.

DG(P_p)	$\mathcal{K}$	**MC value**	**ref. value [16]**	$h = 0.1$	$h = 0.05$	$h = 0.02$	$h = 0.01$
	80	0.26	0.23	0.1927	0.2458	0.2597	0.2612
	90	1.46	1.38	1.3425	1.4339	1.4571	1.4698
$p = 1$	100	4.96	4.86	4.8227	4.9336	4.9634	4.9673
	110	11.52	11.45	11.3274	11.4691	11.5119	11.5188
	120	20.32	20.28	20.1090	20.2538	20.2992	20.3074
	130	30.05	30.03	29.9179	30.0068	30.0331	30.0381
	80	0.26	0.23	0.2575	0.2587	0.2588	0.2588
	90	1.46	1.38	1.4514	1.4525	1.4525	1.4525
$p = 2$	100	4.96	4.86	4.9610	4.9587	4.9579	4.9565
	110	11.52	11.45	11.5124	11.5137	11.5136	11.5135
	120	20.32	20.28	20.3053	20.3076	20.3078	20.3078
	130	30.05	30.03	30.0406	30.0393	30.0393	30.0393
	80	0.26	0.23	0.2588	0.2588	0.2588	0.2588
	90	1.46	1.38	1.4525	1.4525	1.4525	1.4525
$p = 3$	100	4.96	4.86	4.9573	4.9569	4.9472	4.9400
	110	11.52	11.45	11.5128	11.5136	11.5136	11.5136
	120	20.32	20.28	20.3078	20.3079	20.3080	20.3080
	130	30.05	30.03	30.0394	30.0394	30.0395	30.0395

TABLE 2. Comparison of approximate one-year option values at reference node $[S_{ref}, Y_{ref}]$ for different scenarios, mesh sizes and polynomial orders with the reference results.

DG(P_p)	$\mathcal{K}$	**MC value**	**ref. value [16]**	$h = 0.1$	$h = 0.05$	$h = 0.02$	$h = 0.01$
	80	2.65	2.28	2.3987	2.4454	2.4601	2.4628
	90	5.53	5.03	5.2265	5.2847	5.3046	5.3086
$p = 1$	100	9.96	9.42	9.6305	9.6986	9.7221	9.7268
	110	15.96	15.47	15.6267	15.7067	15.7334	15.7386
	120	23.33	22.94	23.0059	23.0980	23.1273	23.1328
	130	31.74	31.46	31.4389	31.5368	31.5672	31.5727
	80	2.65	2.28	2.4542	2.4544	2.4543	2.4543
	90	5.53	5.03	5.2939	5.2938	5.2936	5.2936
$p = 2$	100	9.96	9.42	9.7065	9.7062	9.7058	9.7055
	110	15.96	15.47	15.7133	15.7130	15.7128	15.7127
	120	23.33	22.94	23.1044	23.1043	23.1042	23.1041
	130	31.74	31.46	31.5429	31.543	31.5429	31.5428
	80	2.65	2.28	2.4540	2.4541	2.4541	2.4541
	90	5.53	5.03	5.2933	5.2933	5.2934	5.2934
$p = 3$	100	9.96	9.42	9.7045	9.7046	9.7045	9.7036
	110	15.96	15.47	15.7125	15.7126	15.7126	15.7126
	120	23.33	22.94	23.1041	23.1042	23.1042	23.1042
	130	31.74	31.46	31.5430	31.5431	31.5431	31.5431

CONCLUDING REMARKS

In this contribution we have extended our previous results [11, 12] related to the numerical approximation of a European-style option value via the DG numerical scheme with stochastic volatility. In particular, we have considered the modified Scott model, which uses the exponential Ornstein–Uhlenbeck process to capture returns volatility dynamics and in this way can be regarded as an alternative to Heston and Stein–Stein stochastic volatility models. The comparative numerical experiments show quite good accordance with reference values (theoretically correct price obtained via MC simulation) and overcome selected benchmarks. Obviously, the proposed scheme can be further extended to deal with other options and processes in order to fully utilize the advantages of the DG approach; however, in such cases it is not so easy to obtain benchmarks for the comparison.

ACKNOWLEDGMENTS

Both authors were supported through the Czech Science Foundation (GAČR) under project 16-09541S. The support is greatly acknowledged. Furthermore, the second author also acknowledges the support provided within SP2018/34, an SGS research project of VŠB-TU Ostrava.

REFERENCES

[1] F. Black and M. Scholes, Journal of Political Economy **81**, 637–654 (1973).
[2] R. Merton, Bell Journal of Economics and Management Science **4**, 141–183 (1973).
[3] R. Seydel, *Tools for computational finance* (Springer-Verlag, Berlin, 2009).
[4] J. Topper, *Financial Engineering with Finite Elements* (Wiley, 2005).
[5] B. Rivière, *Discontinuous Galerkin Methods for Solving Elliptic and Parabolic Equations: Theory and Implementation* (Society for Industrial and Applied Mathematics, Philadelphia, 2008).
[6] V. Dolejší and M. Feistauer, *Discontinuous Galerkin Method – Analysis and Applications to Compressible Flow* (Springer-Verlag, 2015).
[7] D. Černá and V. Finěk, Axioms **6**, 1–21 (2017).
[8] D. Černá and V. Finěk, Results in Mathematics **69**, 225–243 (2016).
[9] D. Černá, Computers & Mathematics with Applications **75**, 3186–3200 (2018).
[10] D. Černá and V. Finěk, Electronic Transactions on Numerical Analysis **48**, 15–39 (2018).
[11] J. Hozman and T. Tichý, "A discontinuous Galerkin method for numerical pricing of European options under Heston stochastic volatility," in *AMEE '16*, AIP Conference Proceedings 1789, edited by V. Pasheva, N. Popivanov, and G. Venkov (American Institute of Physics, Melville, NY, 2016) p. 030003.
[12] J. Hozman and T. Tichý, "A DG approach to the numerical solution of the Stein–Stein stochastic volatility option pricing model," in *AMEE '17*, AIP Conference Proceedings 1910, edited by V. Pasheva, N. Popivanov, and G. Venkov (American Institute of Physics, Melville, NY, 2017) p. 030006.
[13] L. Scott, Journal of Financial and Quantitative Analysis **22**, 419–438 (1987).
[14] J. Hozman and T. Tichý, Journal of Computational and Applied Mathematics **344**, 585–600 (2018).
[15] L. Bergomi, *Stochastic Volatility Modeling* (Chapman and Hall/CRC, Boca Raton, 2016).
[16] J. Perelló, R. Sircar, and J. Masoliver, Journal of Statistical Mechanics: Theory and Experiment **2008**, p. P06010 (2008).
[17] O. Oleinik, *Second Order Equations with Nonnegative Characteristic Form* (American Mathematical Society, Providence, 1973).
[18] J. Hozman and T. Tichý, Filomat **30**, 4253–4263 (2016).
[19] J. Hozman and T. Tichý, Applications of Mathematics **62**, 607–632 (2017).
[20] F. Hecht, Journal of Numerical Mathematics **20**, 251–265 (2012).